Desalination and Water Treatment
www.deswater.com

18 (2010) 277–285
June

1944-3994 / 1944-3986 © 2010 Desalination Publications. All rights reserved.
doi: 10.5004/dwt.2010.1785

Simulation and mechanisms of aeration impacts on the permeate flux in submerged membrane systems

Xiaoling Lei

Professor, School of River and Ocean Engineering, Chongqing Jiaotong University, No.66, Xuefu Road, Nanan District, Chongqing, China 400074
email: ellenlei2002@yahoo.com, ellenlei2008@126.com

Received 3 June 2009; Accepted 29 December 2009

ABSTRACT

This study was designed to investigate the impacts and mechanisms of aeration of the liquid crossflow along membrane surface, and the air bubble contact with membrane surface on the permeate flux in a submerged membrane system. The results indicate that the decline of the permeate flux over filtration time and filtered volume could be characterized by an initial short period of fast permeate flux decline, followed by a longer period of slower permeate flux decline, according to an exponential equation. Aeration had a great impact on enhancing the permeate flux. The maximum pseudo-steady state permeate flux and the minimum pseudo-steady-state permeate flux decline coefficient were achieved when the membrane system was operated with aeration. Aeration had a significant impact on the pseudo-steady-state permeate flux and the pseudo-steady-state permeate flux decline coefficient. As the intensity of aeration increased, the pseudo-steady-state permeate flux increased, and the pseudo-steady-state permeate flux decline coefficient decreased. However, there were no significant meanings in pseudo-steady-state permeate flux and pseudo-steady-state permeate flux decline coefficient if the aeration intensity is operated too high. Throughout this study, a better knowledge of aeration impacts and mechanisms are gained, and the submerged membrane systems could be designed and operated so as to maximize the permeate flux.

Keywords: Submerged membrane system; Aeration; Permeate flux; Impacts; Simulation; Mechanisms

1. Introduction

Since the development of synthetic asymmetric membranes in 1960, membrane processes for water and wastewater treatment have grown steadily. Moreover, the hollow-fiber microfiltration (MF) and ultrafiltration (UF) membrane processes have had the most profound impact on the use, acceptance, and regulation of all types of membrane processes for drinking water treatment [1]. The use of submerged membrane processes has increased rapidly for drinking water treatment applications. However, the operating costs for submerged membrane systems are still relatively high, when compared with conventional treatment technologies, such as sand filtration. The capital and operating costs associated with membrane systems are typically proportional to the membrane permeate flux that can be achieved. Thus, the permeate flux, which can be achieved, and the factors that affect the permeate flux are central considerations in determining membrane performance and cost. Moreover, the permeate flux that can be achieved is largely governed by the extent of fouling that occurs on the membrane surface.

The impacts of aeration on confined membrane systems have been extensively investigated and presented by Cui et al. [2]. As with their confined counterparts, unconfined membrane systems are also significantly influenced by aeration. However, in an unconfined system, such as a submerged hollow fiber membrane system, other mechanisms can also potentially contribute to the high shear forces that are generated at a membrane surface, notably the shear forces resulting from the swaying of a membrane fiber in the wake of an air slug [3]. As a result, the relative contribution of these mechanisms on the resulting improvements in permeate flux is unknown, and the impact of aeration on submerged hollow fiber systems is poorly understood.

This study was designed to address the current knowledge gap and undertaken to investigate and simulate the impacts and mechanisms of aeration, the liquid crossflow along membrane surface, and the air bubble contact with membrane surface on the permeate flux in a submerged membrane system. Throughout this study, a better knowledge of aeration impacts and mechanisms will enable submerged member systems to be designed and operated to maximize the permeate flux.

2. Permeate flux and aeration in membrane system

2.1. Material accumulation and permeate flux decline in membrane system

The permeate flux (Jv) of clean water across a membrane can be estimated using Darcy's law [4].

$$Jv = \frac{\Delta P}{\mu * Rm} \tag{1}$$

where, ΔP is the transmembrane pressure [N/m^2]; μ is the absolute viscosity of the water being filtered [$N{\cdot}s/m^2$]; and Rm is the hydraulic resistance of the clean membrane to permeate flow [$N{\cdot}s/m^3$].

However, when a liquid matrix is filtered, the materials accumulate on and within the membrane by blocking or constricting pores and by forming a layer. Over time, the retained materials can accumulate at the membrane surface. Material accumulation, which is also commonly referred to as fouling, may arise from particle deposits on the membrane surface, macromolecules adsorbing onto the membrane surface, or within the membrane pores. As a result, the membrane resistance to the permeated flow increases over time. For a given operating transmembrane pressure and liquid matrix, an increase in the resistance due to the accumulation of retained material results in a decline in the permeate flux, as suggested by Eq. 2 [5,6].

$$Jv = \frac{\Delta P}{\mu * (Rm + Rr)} \tag{2}$$

where Rr is the hydraulic resistance caused by retained material to permeate flow [$N{\cdot}s/m^3$].

Considering that materials that accumulate on the membrane surface increases over time, the permeate flux through a membrane decreases over time. Earlier studies by Hermia (1982) have shown that the decline in the permeate flux occurs in two stages [5]. The initial stage is characterized by a short term rapid flux decline due to pore blocking and cake formation. The second stage is characterized by a long term gradual flux decline, due to cake compaction precipitative fouling, and/or adsorptive fouling.

The rate at which the permeate flux declines is governed by the rate at which material accumulates at the membrane surface. The rate at which the permeate flux declines can be controlled by varying the magnitude of the shear that is imposed onto the membrane surface. The accumulated materials can also be periodically removed by relaxation and/or backwash cycles.

2.2. Aeration in submerged hollow fiber membrane system

One of the main limitations for membrane system is the permeate flux decline that occurs over time. This decline is associated with the material accumulation on the membrane surface. Aeration is used in submerged membrane systems to minimize the extent of material accumulation on the membrane surface.

Ozaki and Yamamoto (2001) investigated the effects of crossflow velocity induced by aeration on the foulant accumulation process in a bioreactor, using flat-sheet membrane modules [7]. They observed that foulant accumulation rate was initially very low, followed by an increase. Furthermore, the extent of sludge accumulation, the sludge accumulation rate, and the lag phase were dependent on aeration intensity. Therefore, the extent of sludge accumulation and the sludge accumulation rate are significantly impacted by the extent of aeration.

Chang and Fane (2002) investigated the impact of aeration intensity on the vacuum pressure needed to maintain a constant permeate flux in a submerged hollow fiber membrane system [8]. They observed that the extent of the increase in the vacuum pressure (i.e. over time) was lower at higher aeration intensities. They also observed that the beneficial impact of aeration on reducing the extent of the increase in the vacuum pressure plateaus when the aeration intensity was increased above a certain value.

3. Experimental design

This study was conducted using the bench-scale submerged membrane system illustrated in Fig. 1. The laboratory submerged membrane system consists of a

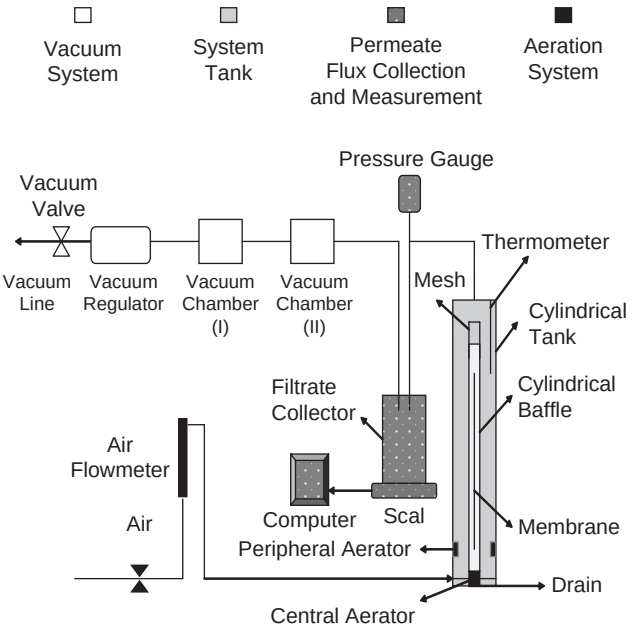

Fig. 1. Schematic of the laboratory set-up.

system tank, membrane modules, an aeration system, a vacuum system, and a permeate flux collection and measurement system.

3.1. Membrane module and source water

The length of the fibers in each membrane module was 0.42 m, with a total effective membrane surface area of 0.0023 m^2. The physical characteristics of the membranes are presented in Table 1 and the configurations of the membrane modules are shown in Fig. 2.

The source water to be filtered in this study was a mixture from a reservoir and a pond. It had a TOC of approximately 10 mg/L, and a relatively higher fouling potential. It was possible to foul the membrane surface significantly (i.e. achieve a significant reduction in the permeate flux) within one to two days.

Table 1
Physical characteristics of the membranes used in the present study.

Configuration	Surface properties	Outside diameter (mm)	Nominal pore diameter (μm)	Typical operating transmembrane pressure (psig)
Outside-in hollow-fiber	Non-ionic & hydrophilic	1.8	0.04	1-8

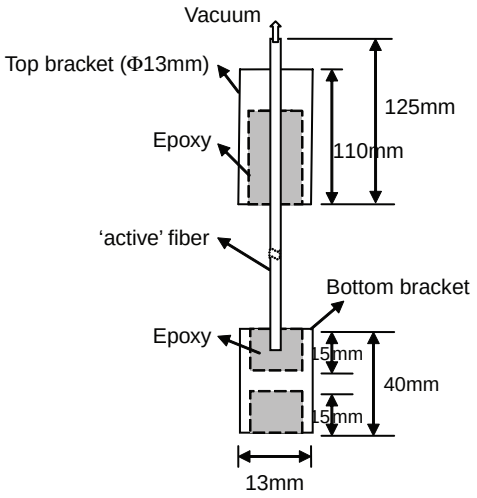

Fig. 2. Schematic of membrane module.

3.2. Permeate flux collection and measurement

The flow measurement system consists of a collection container, a digital electrical scale, and a computer (see Fig. 1). The digital scale (Scout Pro 4000) was used to measure the weight of permeate which accumulated in the collection container over time. The cumulative weight was automatically logged into a computer at one-minute intervals, and automatically connected to a permeate flow rate. Periodically (i.e. every 1 hour), a volume of raw water, equivalent to that which was collected over the past hour, was added to the system tank to maintain a relatively constant liquid level.

3.3. Control of system crossflow

Both single phase (water only) and dual phase (water + aeration) crossflow, along the membrane surface, were studied. Dual phase crossflow along the membrane surface was generated by aerating the system tank with the central diffuser. The rising air bubbles, which were confined to the inside of the cylindrical baffle, entrained water upwards along the inside of the cylindrical baffle. A schematic of the flow path for the dual phase crossflow is illustrated in Fig. 3(a). Single phase crossflow along the membrane surface was generated by aerating the system tank with the peripheral aerator. The rising air bubbles entrained water upwards along the outside of the cylindrical baffle, and subsequently downwards through the inside of the cylindrical baffle. A mesh screen located at the top of the cylindrical baffle ensured that no air bubbles were entrained downwards into the cylindrical baffle. A schematic of the flow path for the single phase crossflow along the membrane surface is illustrated in Fig. 3(b).

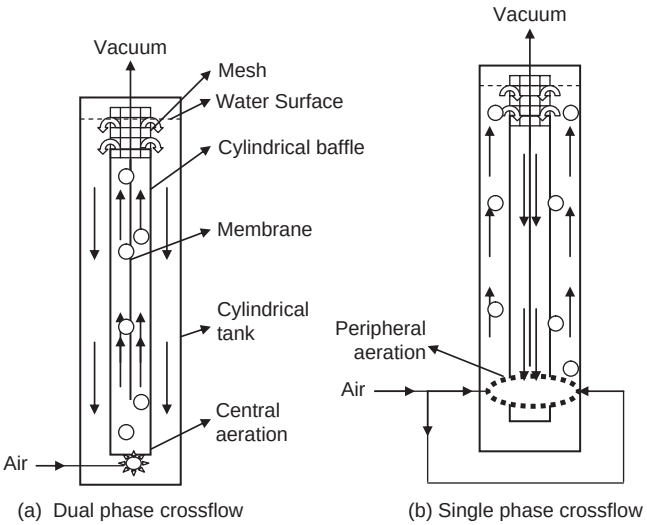

Fig. 3. Schematic of system crossflow (arrows represent direction of bulkflow).

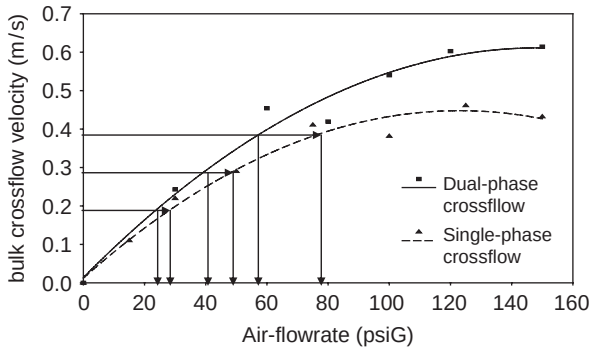

Fig. 4. Relationships between bulk crossflow velocity and air flowrate.

For both single phase and dual phase (with aeration) crossflow operations, the bulk liquid crossflow velocity at the membrane surface could be controlled by varying the flow rate of air into the respective aerators. The relationship between the air flow rate and the bulk crossflow velocity at the membrane surface, for both single phase and dual phase crossflows, is presented in Fig. 4.

For the present study, bulk crossflow velocities of 0, 0.2, 0.3 and 0.4 m/s were considered. The corresponding air flow rates, to achieve these bulk crossflow velocities for both the single phase and the dual phase crossflow systems, are presented in Table 2.

3.4. Experimental series

Three series of experiments were designed to investigate and simulated the impacts and mechanisms of aeration on the permeate flux in a submerged membrane system. Key hydrodynamic conditions of each experiment studied in this research are summarized in Table 3.

Table 2
Operating bulk crossflow velocity and air flowrate.

Bulk crossflow velocity (m/s)	Single phase crossflow system Air flowrate (ml/min)	Dual phase crossflow system Air flowrate (ml/min)
0	0	0
0.2	3800	3200
0.3	6400	5300
0.4	10200	7500

Table 3
Key characteristics of hydrodynamic conditions of each experiment.

Experiment series No.	Purpose of experiments	Experimental condition	Bulk crossflow velocity (m/s)
1	Impact of single phase crossflow on permeate flux	single phase (water only) crossflow along membrane surface	0.2 0.3 0.4
2	Impact of aeration on permeate flux	dual phase (with aeration) crossflow along membrane surface	0.2 0.3 0.4
3	Datum condition	Static water	0

4. Impacts of aeration on permeate flux

4.1. Permeate flux decline over time

The results for all of the series of experiments are presented in terms of permeate flux versus filtration time. The following overall trends can be observed.

1. For all experimental conditions, the permeate flux initially decreased rapidly.
2. The rate of initial rapid decrease in the permeate flux increased in the following order: experimental series with aeration; experimental series with single phase crossflow; and experimental series with static conditions.
3. True steady state conditions were never reached. For all experimental conditions, the permeate flux

continued to slowly decrease over time after the initial rapid decrease. The magnitude of the permeate flux, following the initial period of rapid decrease, was defined as the pseudo steady state permeate flux.
4. For all experimental conditions, pseudo steady state conditions were reached at approximately 260 minutes after the start of the filtration experiment.
5. The magnitude of pseudo steady state permeates flux for the different experimental conditions increased in the following order: experimental series with static conditions; experimental series with single phase crossflow; and experimental series with aeration.

4.2. Permeate flux decline with volume filtered

As suggested by Hermia, depending on the type of fouling, the extent of the decline in the permeate flux can be related to the amount of permeate filtered, rather than the filtration time [5]. The results for all of the series of experiments are presented in terms of permeate flux versus volume filtered. The following overall trends were observed:

1. The trend observed for the permeate flux versus volume filtered is relatively similar to that observed for the permeate flux versus filtration time.
2. For all experimental conditions, the permeate flux initially decreased rapidly.
3. The rate of initial rapid decrease in the permeate flux increased in the following order: experimental series with aeration crossflow; experimental series with single phase crossflow; and experimental series with static conditions.
4. True steady state conditions were never reached. For all experimental conditions, the permeate flux continued to slowly decrease over time after the initial rapid decrease. The magnitude of the permeate flux, following the initial period of rapid decrease, was defined as the pseudo steady state permeate flux.
5. For all experimental conditions, pseudo steady state conditions were reached approximately when 0.7L filtrate filtered.
6. The magnitudes of pseudo steady state permeate flux for the different experimental conditions increased in the following order: experimental series with static conditions; experimental series with single phase crossflow; and experimental series with aeration crossflow.

5. Simulation of the impacts of aeration on permeate flux

5.1. Proposed formulation for permeate flux decline equation

A number of empirical equations were fitted to the collected data using linear regression. The best fit was observed for an experimental equation of the form, presented below.

$$Jv = c^{*}exp^{-a(t,\,V)} + d^{*}exp^{-b(t,\,V)} \quad (3)$$

where, Jv is the permeate flux [L/m^2·hr]; a, b, c and d are empirical constants; and t and V are the filtration time and the filtration volume, respectively.

Equation 3 was fitted to the data collected in the present study, with respect to both the cumulative filtration time and the cumulative filtration volume. As presented in Table 4, fitting Eq. 3 with respect to the cumulative volume filtered, typically resulted in better results. As a result, the decline in the permeate flux was modeled with respect to the cumulative filtration volume in this study.

The first term on the right hand side of Eq. 3 corresponds to the initial rapid permeate flux decline phase. Field et al. and Hermia also reported that, depending on the fouling mechanism, the decline in the permeate flux can follow an exponential relationship [5,6]. Field et al. indicated that the magnitude of the decline in the permeate flux can be proportional to the difference between the initial permeate flux (J_0) and the steady state (or critical) permeate flux (Jss) [6]. However, the relationships developed by Field et al. assume that steady state conditions can be reached. Once a steady state condition was reached, the permeate flux remained constant [6]. Based on this relationship, the second term on the right hand side of Eq. 3 is constant at the steady state permeate flux. However, true steady state conditions were never reached in the present study. For the present study,

Table 4
Multiple coefficients of determination for experimental results using Eq. 3.

Experiment series No.	Bulk crossflow velocity (m/s)	Value of multiple coefficient of determination (I^2) for non-linear regression analysis using Eq. 3	
		Jv versus t	Jv versus V
1	0.2	0.9852	0.9850
	0.3	0.9323	0.9333
	0.4	0.9198	0.9097
2	0.2	0.9901	0.9948
	0.3	0.9536	0.9587
	0.4	0.9486	0.9495
3	0	0.9793	0.9953

the magnitude of the decline in the permeate flux that occurs during the initial phase was defined as the difference between the initial permeate flux and the pseudo-steady-state permeate flux (*J'ss*). The rate of the decline in the permeate flux that occurs during the initial phase was defined by an exponential coefficient (*a*).

The second term on the right hand side of Eq. 3 corresponds the subsequent long-term slow permeate flux decline along with the initial rapid permeate flux decline. The magnitude of the decline that can occur in this phase was defined as the pseudo-steady-state permeate flux. The rate of the decline in the permeate flux, during the long-term permeate flux decline, was defined in terms of the pseudo steady state permeate flux reduction coefficient (*b*). The resulting modifications to Eq. 3 are presented in Eq. 4.

$$Jv = (Jo - J'ss) * exp^{-aV} + J'ss * exp^{-bV} \quad (4)$$

where, *Jv* is the permeate flux [L/m^{2}hr]; *Jo* is the initial permeate flux [L/m^{2}hr]; *J'ss* is the pseudo-steady-state permeate flux [L/m^{2}hr]; *a* is the initial permeate flux decline coefficient [L^{-1}]; *b* is the pseudo-steady-state permeate flux decline coefficient [L^{-1}]; and *V* is the filtration volume [L].

It should be noted that all of the experimental measurements are within a 99% confidence interval associated with the fit of Eq. 4 to the collected data.

5.2. Parameter estimation

The absolute values associated with the pseudo-steady-state permeate flux, the initial permeate flux decline coefficient and the pseudo-steady-state permeate flux decline coefficient were used to measure and assess the magnitude of the impact of aeration conditions on the permeate flux.

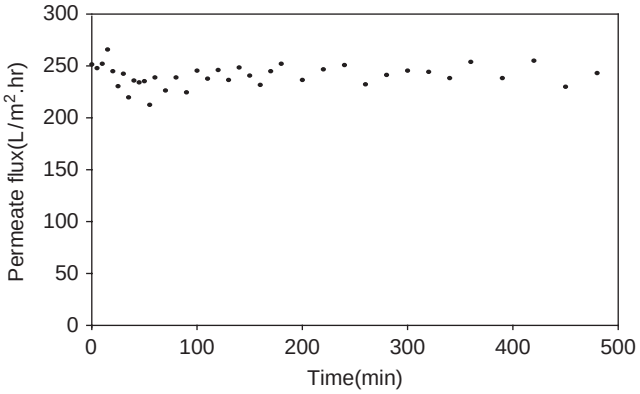

Fig. 5. Estimate of the Initial Permeate Flux.

The initial permeate flux is the permeate flux through a membrane in the absence of any fouling. The initial permeate flux was measured using a clean membrane when filtering clean water (distilled water) under the typical experimental condition as a transmembrane pressure of 4.1psi (27.7kPa) and the liquid temperature of 25°C. The values obtained for the initial permeate flux are shown in Fig. 5 and the initial permeate flux was determined to be 240.5 L/m^{2}hr for the present study. All permeate flux data collected during the present study was normalized to the same experimental condition as a transmembrane pressure of 4.1psi (27.7kPa) and the liquid temperature of 25°C.

Non-linear regression was used to fit Eq. 4 to the experimental data. The resulting estimates for the pseudo-steady-state permeate flux, the initial permeate flux decline coefficient and the pseudo-steady-state permeate flux decline coefficient are summarized in Table 5.

Table 5
Estimate of the pseudo-steady-state permeate flux, the initial permeate flux decline coefficient and the pseudo-steady-state permeate flux decline coefficient.

Experiment series No.	Bulk crossflow velocity (m/s)	Pseudo-steady-state permeate flux(J'ss) (L/m^2.hr)	Initial permeate flux decline coefficient(a) (L^{-1})	Pseudo-steady-state permeate flux decline coefficient(b) (L^{-1})
1	0.2	42.9 ± 1.68	8.39 ± 0.27	0.673 ± 0.045
	0.3	38.0 ± 4.47	8.28 ± 0.97	0.463 ± 0.120
	0.4	44.2 ± 1.29	7.77 ± 0.32	0.359 ± 0.025
2	0.2	65.0 ± 1.30	5.36 ± 0.17	0.235 ± 0.014
	0.3	91.8 ± 4.24	7.78 ± 1.12	0.309 ± 0.049
	0.4	93.7 ± 1.00	5.36 ± 1.31	0.268 ± 0.096
3	0	25.7 ± 1.29	6.93 ± 0.16	0.839 ± 0.043

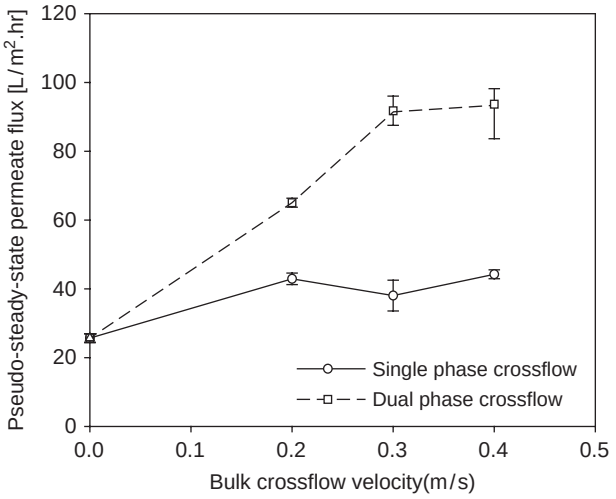

Fig. 6. Relationship of pseudo-steady-state permeate flux and aeration intensity (Error bars represent the standard error of the estimated parameter).

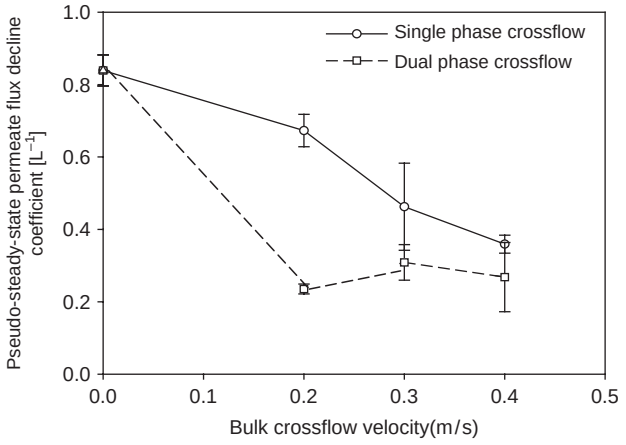

Fig. 7. Relation of the pseudo-steady-state permeate flux decline coefficient with aeration intensity (Error bars represent the standard error of the estimated parameter).

6. Discussion of the results

6.1. Relationship between the pseudo-steady-state permeate flux and aeration intensity

The results of aeration on the pseudo-steady-state permeate flux agree very well as summarized in Fig. 6.

Based on the results presented in Fig. 6, the following observations can be made.First, aeration enabled a high pseudo-steady-state permeate flux to be maintained. The maximum pseudo-steady state permeate flux that could be reached with aeration (i.e. dual phase crossflow at the crossflow velocity of 0.4m/s) was approximately 135% higher than that which could be achieved without aeration (i.e. single phase crossflow at the crossflow velocity of 0.4 m/s), and approximately 264% higher than that which could be achieved under statistic condition (at the bulk crossflow velocity of 0m/s). Therefore, to maximize the pseudo-steady-state permeate flux, the membrane should be operated with aeration under dual phase crossflow.

Second, the bulk crossflow velocity with aeration had a significant impact on the pseudo-steady-state permeate flux. As the dual phase crossflow velocity increased, the pseudo-steady-state permeate flux increased. At a bulk crossflow velocity of 0.2 m/s, the pseudo-steady-state permeate flux with aeration was 52% higher compared with that under single phase crossflow, and 153% higher compared with that at 0 m/s. At 0.3 m/s, the pseudo-steady-state permeate flux with aeration was further enhanced to be 118% higher compared with that under single phase crossflow, and 257% higher compared to that at 0 m/s.

Third, there was no significant difference in the pseudo-steady-state permeate flux for dual phase bulk crossflow velocities of 0.3 m/s and 0.4 m/s. Therefore, there were no significant meanings in pseudo-steady-state permeate flux for aeration bulk crossflow velocities in excess of 0.3m/s.

6.2. Relationship between the pseudo-steady-state permeate flux decline coefficient and aeration intensity

The results of aeration on the pseudo-steady-state permeate flux decline coefficient agree very well as summarized in Fig. 7.

Based on the results presented in Fig. 7, the following observations can be made.First, aeration enabled a lower pseudo-steady-state permeate flux decline coefficient to be maintained. The minimum pseudo-steady-state permeate flux decline coefficient that could be reached with aeration (i.e. dual phase crossflow at the crossflow velocity of 0.4 m/s) was approximately 70% less than that which could be achieved under statistic condition (at the bulk crossflow velocity of 0 m/s), and approximately 25% less than that which could be achieved under single phase crossflow condition (at the bulk crossflow velocity of 0.4 m/s). Therefore, to minimize the pseudo-steady-state permeate flux decline coefficient, the membrane should be operated with aeration under dual phase crossflow.

Second, the bulk crossflow velocity with aeration had a significant impact on the pseudo-steady-state permeate flux decline coefficient. As the dual phase crossflow velocity increased, the pseudo-steady-state permeate flux decline coefficient decreased. At a bulk crossflow velocity of 0.2 m/s, the pseudo-steady-state permeate flux decline coefficient with aeration was 65% lower compared to that under single phase crossflow, and 72% lower compared to that at 0 m/s.

Third, however there was no significant difference in the pseudo-steady-state permeate flux decline coefficient for dual phase bulk crossflow velocities of 0.2 m/s, 0.3 m/s and 0.4 m/s. Therefore, there was no significant meaning in pseudo-steady-state permeate flux for aeration bulk crossflow velocities in excess of 0.2 m/s.

6.3. Relationship between the pseudo-steady-state permeate flux decline coefficient and the pseudo-steady-state permeate flux

Further numerical analysis revealed that the pseudo-steady-state permeate flux decline coefficient may be related to the pseudo-steady-state permeate flux. As presented in Fig. 8, the pseudo-steady-state permeate flux decline coefficient was proportional to the inverse of pseudo-steady-state permeate flux (1/J'ss) for all of the experimental conditions investigated in this present study. The inverse of pseudo-steady-state permeate flux is proportional to the time that the permeating liquid spends in a membrane pore.

Equation 4 was modified to include the linear relationship between pseudo-steady-state permeate flux decline coefficient and pseudo-steady-state permeate flux as presented in Eq. 5.

$$Jv = (J_o - J'ss) * exp^{-aV} + J'ss * exp^{-b'V/J'ss} \quad (5)$$

where, b' is a modified pseudo-steady-state permeate flux decline coefficient and is equal to 21.44 $m^{-2}hr^{-1}$ for the experimental conditions considered in the present study and the standard error of the estimates is 2.141.

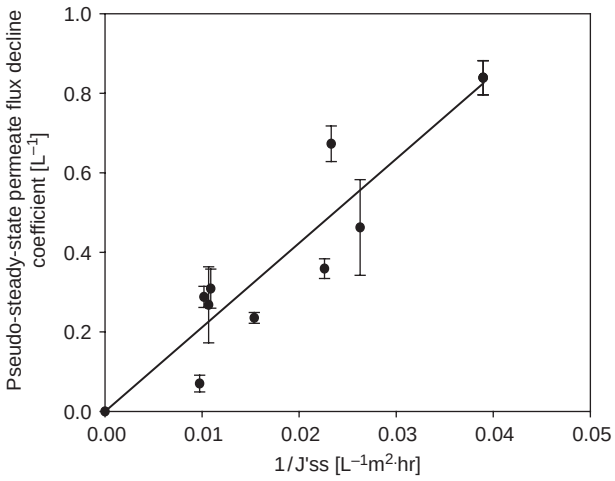

Fig. 8. Relation of pseudo-steady-state permeate flux decline coefficient with the inverse of pseudo-steady-state permeate flux.

If the modified pseudo-steady-state permeate flux decline coefficient is related to the rate of adsorption of foulants on to the surface of a membrane pore, it would be expected to be impacted by the characteristics of the raw water being filtered. Similarly, the modified pseudo-steady-state permeate flux decline coefficient would also be expected to be impacted by pre-treatment processes (e.g. pre coagulation) that would impact the raw water characteristics. Further studies are required to identify the raw water characteristics and pre-treatment processes that can potentially impact the modified pseudo-steady-state permeate flux decline coefficient.

7. Conclusions

Throughout this study, the following conclusions are drawn.

For all experimental conditions, the permeate flux initially decreased rapidly, and continued to slowly decrease over filtration time and filtration volume after the initial rapid decrease. True steady state conditions were never reached.

For all experimental conditions, the rate of permeate flux decrease increased in the following order: experimental series with aeration; experimental series with single phase crossflow; and experimental series with static conditions. Meanwhile, the magnitudes of pseudo-steady-state permeate flux for the different experimental conditions increased in the following order: experimental series with static conditions; experimental series with single phase crossflow; and experimental series with aeration.

The decline of the permeate flux both over filtration time and the cumulative filtration volume could be simulated by an initial short period of fast permeate flux decline, followed by a longer period of slower permeate flux decline according to the equation: $Jv = (Jo\text{-}J'ss) * exp^{-a(t,V)} + J'ss * exp^{-b(t,V)}$

In general, aeration had a significant impact on the permeate flux. Aeration enabled a high pseudo-steady-state permeate flux and a lower pseudo-steady-state permeate flux decline coefficient to be maintained.

The intensity of aeration had a significant impact on the permeate flux. As the dual phase crossflow velocity increased, the pseudo-steady-state permeate flux increased, and the pseudo-steady-state permeate flux decline coefficient decreased. However, there were no significant meanings on permeate flux if the bulk crossflow velocities with aeration is operated too high.

The pseudo-steady-state permeate flux decline coefficient was proportional to the inverse of pseudo-steady-state permeate flux for all of the experimental conditions investigated in this present study. The decline of the per-

meate flux over time was modified to be the equation: $Jv = (Jo–J'ss) * exp^{-aV} + J'ss * exp^{-b'V/J'ss}$

Acknowledgements

The experiments of this work were conducted at the Department of Civil Engineering, University of British Columbia.

The organization of this paper was supported by Ministry of Human Resources and Social Security of the People's Republic of China.

References

[1] EPA, Membrane Filtration Guidance Manual, 815-D-03-008, 2003.
[2] Z.F. Cui, S. Chang and A.G. Fane, The use of gas bubbling to enhance membraneen processes, J. Membr. Sci., 121(1) (2000) 1.
[3] C. Cabassud, S. Laborie, L. Durand-Bourlier and J.M. Laine, Air sparging in ultrafiltration hollow fibers: relationship between flux enhancement, cake characteristics and hydrodynamic parameters, J. Membr. Sci., 181(1) (2001) 57.
[4] J. Mallevialle, P.E. Odendaal and M.R. Wiesner, Water Treatment Membrane Processes, McGraw-Hill, 1996.
[5] J. Hermia, Constant Pressure Blocking Filtration Laws-Application to Power-law Non-Newtonian Fluids, Institut de Genie Chimique UCL, Louvain –la-Neuve, Belgium, 1982.
[6] R.W. Field, D. Wu, J.A. Howell and B.B. Gupta, Critical flux concept for microfiltration fouling, J. Membr. Sci., 100 (1995) 259.
[7] N. Ozaki and K. Yamamoto, Hydraulic effects on sludge accumulation on membrane surface in crossflow filtration, Water. Res., 35(13) (2001) 3137.
[8] S. Chang and A.G. Fane, Filtration of biomass with laboratory-scale submerged hollow fibre modules–effect of operating conditions and module configuration, J. Chem. Technol. Biotechnol., 77 (2002) 1030.